RSC Advances

ROYAL SOCIETY OF CHEMISTRY

www.rsc.org/advances

Toughened redox-active hydrogel as flexible electrolyte and separator applying supercapacitors with superior performance

Enke Feng[a], Guofu Ma*[a], Kanjun Sun[b], Qian Yang[a], Hui Peng[a], Ziqiang Lei*[a]

[a]*Key Laboratory of Eco-Environment-Related Polymer Materials of Ministry of Education, Key Laboratory of Polymer Materials of Gansu Province, College of Chemistry and Chemical Engineering, Northwest Normal University, Lanzhou 730070, China.*

[b]*College of Chemistry and Environmental Science, Lanzhou City University, Lanzhou 730070, China.*

*Corresponding authors. Tel./Fax.: +86 931 7975121

E-mail addresses: magf@nwnu.edu.cn (G. Ma), leizq@nwnu.edu.cn (Z. Lei).

Abstract

Gel electrolytes with reasonable ionic conductivity and high mechanical strength have drawn great interest for applications in flexible and wearable devices. However, the demands for gel electrolytes that combine high mechanical strength and excellent electrochemical performances remain a challenge. Here, a novel redox-active gel electrolyte was prepared by adding AQQS (1-anthraquinone sulfonic acid sodium) to PVA (polyvinyl alcohol)-H_2SO_4 system using a simple solution-mixing/casting method, which possesses not only excellent mechanical strength but also a high ionic conductivity of 28.5 mS cm^{-1}. Surprisingly, the as-fabricated supercapacitor can be operated at a wide voltage range of 0~1.4 V, which is much larger than that of the previously reported active electrolyte based supercapacitors (about 1.0 V). Furthermore, the supercapacitor exhibits superior electrochemical performance such as a maximum specific capacitance of 448 F g^{-1} at a current density of 0.5 A g^{-1}, a considerably high specific energy of 30.5 Wh kg^{-1} at a specific power of 350 W kg^{-1} and good cycling stability with 91% specific capacitance retention

after 1000 cycles. Additionally, such device displays remarkably stable capacitive performance when the gel electrolyte even under a large tensile strain of 100%, a high pressure of 2000 kPa or fold states. The results doubtlessly demonstrates that the toughened redox-active gel polymer is a promising electrolyte candidate in developing high energy density flexible energy storage devices.

1. Introduction

Flexible electronics, which have the ability to endure large levels of strain without remarkable loss in their electronic performance and reliability,[1-3] have attracted more attention due to wide applications.[4-7] Among different energy-storage devices, supercapacitors are important because of their higher power density, long cycle life, and high charge/discharge rates as against that of batteries.[8-10] Concerning flexible supercapacitors, the current research is mainly focused on the fabrication of high-performance flexible electrode materials, such as free-standing carbon films (e.g., carbon fiber,[11] CNT,[12] graphene[13] or MXene-carbon[14] and their composites with conducting polymers[15] and metal oxides[16] or soft substrate (e.g., paper,[17] cloth,[18] sponge,[19] and plastic) supported electrodes.

However, the electrolyte is also a critical factor that determines the performance of flexible supercapacitors, which usually involves liquid (aqueous and nonaqueous) and solid-state forms.[20,21] Solid-state electrolytes are preferred in flexible supercapacitors because of their advantages in terms of the compactness, reliability, and freedom from liquid leakage. Compared with dry solid-polymer electrolytes (10^{-8} to 10^{-7} S cm^{-1}), gel polymer electrolytes exhibit higher ionic conductivity of 10^{-4} to 10^{-1} S cm^{-1} under ambient conditions, which are actually quasi-solid-state electrolytes composed of a polymeric framework, with an organic/aqueous solvent as the dispersion medium and a supporting electrolytic salt/acid/alkali.[22] Unfortunately,

similar to the above hydrogel polymer electrolytes have lower specific capacitances and energy densities, which is a major drawback for the large scale application and prohibitive to many mobile technologies.[23]

An efficient strategy to achieve the gel polymer electrolytes with outstanding electrochemical performance has recently been developed through the introduction of redox additives into the gel polymer systems. The total specific capacitance and energy density of the supercapacitors are significantly increased as a result of the additional pseudocapacitance originating from the electron transfer redox reaction of the redox additive. Notably, Senthilkumar *et al.*[24] reported that 57.2% of specific capacitance and energy density was increased while introducing Na_2MoO_4 (sodium molybdate) as the redox mediator in PVA-H_2SO_4 gel electrolyte due to the redox reaction between Mo(VI)/Mo(V) and Mo(VI)/Mo(IV) redox couples in PVA-H_2SO_4-Na_2MoO_4 gel electrolyte. Yu *et al.*[25] have reported that added the I^-/I_2 redox couple in the PVA-KOH gel electrolyte. The specific capacitance of the supercapacitor is 236.90 F g^{-1}, increasing by 74.28% compared to the system without KI. Good properties for those electrolytes and supercapacitors inspire us to search for a more stable and efficient redox mediator for high-performance supercapacitors. But, it is worth noticing that the redox-active gel electrolytes with various strain states effect on the capacitive performance of the supercapacitors have not been evaluated in all these reports, yet is highly relevant to develop high energy density flexible energy storage devices.

Herein, a high-performance redox-active gel electrolyte was prepared by adding AQSS (1-anthraquinone sulfonic acid sodium) to PVA (polyvinyl alcohol)-H_2SO_4 system, and it was assembled with activated carbon electrodes to form a supercapacitor. The electrochemical properties and pseudocapacitive effects of as-fabricated supercapacitors were investigated in detail

by cyclic voltammetry, galvanostatic charge-discharge and electrochemical impedance spectroscopy techniques. Moreover, we also evaluated the gel electrolytes with various strain states (stretching, folding and compressing) effect on the capacitive performance of the supercapacitors.

2. Experimental

2.1. Materials

Polyvinyl alcohol (PVA, Aladdin Co., China, molecular weight 44.05 MW, alcoholysis: 99.8-100%), 1-anthraquinone sulfonic acid sodium (AQSS, Aladdin Co., China), H_2SO_4 (Sinopharm Chemical Reagent Co., China). Activated carbon (AC, specific surface area of 2000 $m^2\ g^{-1}$) was purchased from Shanghai Sino Tech Investment Management Co., China, and used without further purification. All other chemical reagents were in analytical grade.

2.2. Preparation of redox-active gel electrolytes

A series of redox-active PVA-H_2SO_4-AQSS gel polymer electrolytes were obtained using a simple solution-mixing/casting method according to different redox additives loading amounts. Typically, 1 g of PVA was dissolved in 20 mL 1 M H_2SO_4 solution under agitation at 85 °C for 2 h. Then, a certain amount of AQSS was added into the above transparent viscous solution. After a homogeneous colloidal substance appeared, the mixture was poured into a plastic petri dish (Φ 9 cm), and frozened at -25 °C for 24 h. Finally, after thawing, the thickness of 1.5 mm round free-standing PVA-H_2SO_4-AQSS gel film was formed. For comparison, PVA-H_2SO_4 without AQSS gel film was also prepared using the same method. The PVA-H_2SO_4 and PVA-H_2SO_4 with 0.1 g AQQS gel films are named as PH and PHA, respectively.

2.3. Preparation of activated carbon electrode and assemble of supercapacitors

Initially, activated carbon (AC), acetylene black and polyvinyl pyrrolidone (PVP) with the mass ratio of 80:10:10 were dispersed in appropriate amount of *N*-methyl-2-pyrrolidone (NMP) at room temperature and stirred continuously to form homogeneous slurry. After that, the slurry was coated on carbon cloth strips (10 mm width × 20 mm length × 0.1 mm thickness), and the electrodes were dried at 120 °C for 12 h and then weighted. The total mass of active material (including acetylene black and polyvinyl pyrrolidone) on each electrode was between 3 and 4 mg, and two electrodes with identical or very close weights were selected for the measurements.

A pair of AC electrodes were placed on both sides of the PHA gel film (10 mm width × 20 mm length × 1.5 mm thickness) to form a two-electrode in a sandwich configuration, where the gel film simultaneously acted as a separator and the electrolyte. Subsequently, a plastic film was used to encapsulate the sandwich configuration, with silicone glue as adhesion agent. However, for commercialization these fabrication methods need to be improved.

2.4. Electrochemical measurements

The electrochemical properties of the fabricated devices were investigated by cyclic voltammetry (CV), galvanostatic charge/discharge (GCD), and electrochemical impedance spectroscopy (EIS) measurements using a CHI 760E electrochemical workstation (Shanghai Chenghua instrument Co., Ltd., China). The cycle-life stability was performed using computer controlled cycling equipment (CT2001A, Wuhan Land Electronics Co., Ltd., China). EIS tests were carried out at open circuit potential with the frequency ranges from 100 mHz to 100 kHz and the data were fitted using ZView software. The equivalent series resistance (*ESR*, Ω) and ionic conductivity (σ, mS cm^{-1}) of gel polymer can be estimated by the following equations:[26,27]

$$ESR = IR_{drop} / 2I \quad (1) \qquad \sigma = L / R S \quad (2)$$

where I (A) is the constant current, IR_{drop} (V) is defined as the electrical potential difference between the two ends of a conducting phase during charging-discharging, L (cm) is the distance between the two electrodes, R (ohm) is the resistance of gel electrolytes and S (cm^2) is the geometric area of the electrode|electrolyte interface.

3. Results and discussions

The morphologies of the activated carbon were examined with field emission scanning electron microscopy (FE-SEM, Carl Zeiss Ultra Plus, Germany) at an accelerating voltage of 5.0 kV. As shown in Fig. 1, the activated carbon material looks composed of irregular surface with loose nanostructures, and has some pores in the macroscopic scale, which makes ionic diffusion easy from bulk electrolyte into the inner space of carbon materials. The mechanical properties of prepared PHA gel polymer were evaluated by stretching, twisting and compressive stress-strain measurements under proper forces, as shown in Fig. 2a, b and c. The PHA gel polymer shows high toughness and good strength when it underwent large deformations, such as which can sustain up to 400% stretching and compressing strains. Meanwhile, when the external force is unloaded, all the gel samples can be restored to its original length and shape. Moreover, it can be seen that the PHA gel polymer still possesses excellent mechanical strength after electrochemical tests (Fig. 2a), which indicates that the PHA gel polymer as an electrolyte and separator material has a good prospect in the flexible energy storage devices application field. Whereas, most hydrogels notably present poor stretchability in previous reports, typically, an alginate hydrogel ruptures when stretched to approximately 120%.[28,29] The schematic diagram of as-fabricated supercapacitor with PHA gel film and its flexible behavior are given in Fig. 2d-f, it can be observed the fabricated supercapacitor can be easy bend and fold.

Fig. 3a shows the cyclic voltammogram (CV) curves of fabricated supercapacitors using 1 M H_2SO_4 aqueous, PH and PHA gel as electrolytes at scan rate of 10 mV s^{-1} in the potential window range from 0 to 1.4 V. The rectangular-like shape CV curve is observed for 1 M H_2SO_4 and PH electrolyte, a clear proof of ideal situation of electrical double layer capacitor, where electrochemical energy is stored by an accumulation of electrolyte ions between the electrodelelectrolyte interfaces. However, the CV curves of supercapacitors in 1 M H_2SO_4 aqueous electrolyte exhibits larger area than that of PH gel electrolyte, meaning that it has a higher specific capacitance. This is attributed to between the activated carbon electrode surface and gel polymer electrolyte lack of better contact in comparison with the liquid electrolyte system. Interestingly, while using PHA as electrolyte and separator, a pair of well-defined and strong redox peaks assigned to the redox reactions of AQQS/H_2AQQS (AQQS + $2H^+$ + $2e^-$ ↔ H_2AQQS) couple appears in the CV curve, which indicates the presence of pseudocapacitance nature.[24] This redox process is clearly seen when comparing a typical supercapacitor with 1 M H_2SO_4 aqueous electrolyte or PH gel electrolyte only exhibiting electrical double-layer capacitance, and the increased enclosed area in the CV curve implies that the capacitance is enhanced. It can therefore be conclude that the total capacitance of the supercapacitor with PHA gel film should be the sum of the electric double-layer capacitance on the surface of activated carbon electrode and the pseudocapacitance produced by redox reactions at the electrodelelectrolyte interface because charging of the electric double layer is accompanied by the redox reactions and both processes work in parallel.[30,31] Fig. 3b presents CV curves for the supercapacitor with PHA gel film at various scan rates. At high scan rate, the supercapacitor exhibits prominent redox peaks when compared with low scan rate that infers the better electrochemical reversibility.[32]

To evaluate the effect of the AQQS amount on the electrochemical behaviour of fabricated supercapacitors, the correlation between the AQQS amounts and the electrode specific capacitance (C_s) of supercapacitors is shown in Fig. 3c. When the amount of AQQS is less than 0.1 g, the C_s of supercapacitors rises quickly and reaches the highest value with the AQQS amount of 0.1 g, then gradually decreases with the increase of AQQS amount, which means that the C_s of supercapacitors can be improved with the appropriate doping amount of AQQS. This result may be due to the fact that the AQQS can act as plasticizer and redox shuttle in the gel polymer. When the AQQS amount is less, the capacitance contribution of a redox process generated by AQQS cannot be realized well at the electrodelelectrolyte interface. However, higher AQQS amount will lead to the aggregation of free ions and the crystallization of AQQS in PH gel system, which impeded the ions transport and induced the decrease of the capacitance.[26] The conclusion can be further confirmed by the impedance spectra, as shown in Fig. 3d. The semicircle intercept in impedance real axis and semicircle diameter of PHA gel film with 0.2 g AQQS is larger than that with 0.1 g AQQS, which results reveal the increased solution resistance and charge transfer resistance when further increasing the AQQS amount. Due to the better electrochemical capacitance behavior of 0.1 g AQQS added into PH system, it is considered as optimal amount for supercapacitors and further studied as follows.

GCD measurements were carried out for the supercapacitors with PH and PHA gel films at the current densities of 0.5 A g^{-1}. As Fig. 4a displays, both supercapacitors show good coulombic efficiency and favourable electrochemical reversibility as that approximately equivalent charge time (T_c) and discharge time (T_d). Interestingly, the supercapacitor with PHA gel film in two potential ranges showed a remarkably smaller IR drop (0.021 V) compared with the PH gel film

(0.065 V). This decreasing IR drop value can improve the performance of supercapacitors, based on the relation $E = 1/8\ C_s\ (V_{initial}$ - IR - $V_{final})^2$. If IR drop is high, energy loss is unavoidable. Additionally, the equivalent series resistance (*ESR*) of supercapacitors is directly proportional to the IR drop according to Eq. (1). So the supercapacitor with PHA gel film obtained the lower ESR value of 2.9 Ω cm^2 (Table 1), confirming the PHA gel film possess a higher ionic conductivity. Futhermore, according to Eq. (2), its ionic conductivity increased by 81.5% up to 28.5 mS cm^{-1} compared to that of PH system. On the other hand, as the redox additives are incorporated into the gel electrolytes, the non-ideal shapes of the GCD curves indicate that the Faradaic contributions to the charge accumulation process.[30] The results are in good accordance with the data obtained from CV.

The charge-discharge curves and the C_s of supercapacitor with PHA gel film at various current densities of 0.5, 1, 1.5, 2 and 3 A g^{-1} are displayed in Fig. 4b and c. The C_s of supercapacitor was calculated by using the formula $C_s = 4\ I\ \Delta t\ /\ M\ \Delta V$,[26] where I (A) is the constant current, Δt (s) is the discharge time, M (g) is the total mass of the active material in both electrodes, and ΔV (V) is the voltage change during the discharge process. Obviously, the supercapacitor with PHA gel film has the higher C_s than the PH gel film at the same current densities, which is consistent with the CV tests. Furthermore, the C_s of supercapacitor with PHA gel film is as high as 448 F g^{-1} at a current density of 0.5 A g^{-1} and 342 F g^{-1} even at a high current density of 3 A g^{-1} (about 76% capacitance retention). The C_s of supercapacitor with PH gel film, by contrast, is just 148 F g^{-1} at a current density of 0.5 A g^{-1}. This enhanced performance can be attributed to the additional pseudocapacitance contribution caused by a quick reversible redox process of AQQS in PHA system at the electrolyte|electrode interfaces, which has been aforementioned.

The Ragone plots of the supercapacitors with PH and PHA gel films describing the relationship between energy density and power density were obtained and are shown in Fig. 4d. The specific energy density (E, Wh kg^{-1}) and power density (P, W kg^{-1}) for a supercapacitor cell were calculated from the discharge curves at different current densities using the following equations: $E = 1/8\ C_s\ \Delta V^2$ and $P = E / \Delta t$,[27] where ΔV (V) is the actual voltage excluding IR drop of the discharge process, and Δt (s) is the discharge time. It is obvious that the supercapacitor with PHA gel film exhibits the highest energy density of 30.5 Wh kg^{-1} with a power density of 350 W kg^{-1} and remained as 23.2 Wh kg^{-1} at 2037 W kg^{-1}, corresponding to an good rate capability. In comparison, at the same power density of 350 W kg^{-1}, the energy density of the supercapacitor with PH gel film is only 10 Wh kg^{-1}. Clearly, the introduction of AQQS redox additives into the PVA-H_2SO_4 gel electrolyte results in a significant enhancement of the energy density of the supercapacitor with PHA gel film by nearly three times. Moreover, the obtained maximum energy density of the supercapacitor with PHA gel film is considerably higher than those of recently reported supercapacitors using redox-active electrolytes (see Table 2). As well as higher than the previously reported asymmetric supercapacitors such as CA//Co_3O_4/NF (17.9 Wh kg^{-1}),[38] MnO_2/NWs/SWNTs//In_2O_3/NWs (25.5 Wh kg^{-1}),[39] CNT/NiO//PCPs (25.4 Wh kg^{-1}),[40] MnO_2/CCNs//CCNs (23.6 Wh kg^{-1})[41] and MnO_2//P-GA (22.8 Wh kg^{-1}).[42]

Fig. 5a shows the Nyquist plots of supercapacitors applying PH and PHA gel films with a small semicircle in the high-frequency region and a vertical curve in the low-frequency region, which indicates a low charge transfer resistance and an excellent capacitive behavior with small diffusion resistance, respectively. The impedance spectra of supercapacitors with PH and PHA gel films were further analyzed by the software of ZSimpWin on the basis of the electrical equivalent

circuit (the inset of Fig. 5a) and fitted impedance parameters are presented in Table 1. Where R_s stands for a combined ohmic resistance of the electrolyte and the internal resistance of the electrode, R_{ct} is the charge transfer resistance caused by the Faradaic reaction. The transition from the semicircle to the long tail of the vertical curve is called the Warburg resistance (W) and is a result of the frequency dependence of ion diffusion/transport in the electrolyte to the electrode surface, C_{dl} is the double-layer capacitance, and C_L is the limitcapacitance.[31] In table 1, it is observed that the decreases of the R_s and R_{ct} of the supercapacitor with PHA gel film indicates that the introduction of AQQS redox additives into PVA-H_2SO_4 gel electrolyte can reduce of internal resistance of the electrolyte and improve the interface nature of gel polymer and electrode material.[29,31] Simultaneously, the decrease in Warburg coefficient suggests that the addition of AQQS redox additives can obtain faster ion diffusion/transport to the electrode surface.[27] Results obtained above are also further confirm that the PHA gel polymer has higher ionic conductivity and much better compatibility with carbon electrodes than the PH. Moreover, The cycling stability test of the supercapacitor with PHA gel film was performed at a current density of 1 A g^{-1} for 1000 galvanostatic charge/discharge cycles, as depicted in Fig. 5b. After 1000 cycles, over 91% capacitance was retained, meaning that the fabricated supercapacitor with the PHA gel film has good electrochemical stability and a high degree of reversibility. The inset shows no significant electrochemical change during the long-term charge-discharge process after cycling 1000 times.

The capacitive performance of the supercapacitor applying PHA gel film with various stretching state (0%, 20%, 40%, 60%, 80% and 100%) was evaluated (Fig. 6a). Surprisingly, the supercapacitor possesses remarkably stable capacitive performance when the PHA gel film under

various stretching state. As shown in the inset of Fig. 6a, the PHA gel film at 0 and 100% stretching strains, the supercapacitor exhibits quite close electrochemical performance with galvanostatic charge/discharge curves almost coinciding with each other, confirming the excellent stretchability of the PHA gel polymer electrolyte. Moreover, the CV curves of the supercapacitor with PHA gel film at flat and fold strains are only very slight deviation (Fig. 6b). And the C_s of supercapacitor with PHA gel film under fold states at various current densities are displayed in Fig. 6c. When the current densities are 0.5, 1, 1.5, 2 and 3 A g^{-1}, the values of C_s are calculated to be 420, 390, 366, 350 and 318 F g^{-1}, which are quite close with supercapacitors under flat states (448, 400, 385, 368 and 342 F g^{-1}). These results indicate that the fabricated supercapacitor can be perfectly bended without affecting the device performance. Meanwhile, when different compressible strains are applied to the supercapacitor with PHA gel film (Fig. 6d), which displays a small capacitance loss of 18% even under a high pressure of 2000 kPa. The outstanding electrochemical properties of PHA gel polymer under various strain states may bring new design opportunities of device configuration for energy-storage devices in the future flexible electronics field.

In general, the total energy stored in a single supercapacitor is too low to meet the practical applications. As a result, several supercapacitors have to be connected together either in series or in parallel to obtain a high specific voltage and current. The electrochemical performance of the series/parallel connection circuit of three supercapacitors with PHA gel film was investigated, as shown in Fig. 7a and b. The CV curve of such a three in-series supercapacitor group (Fig. 7a) exhibits an enhanced potential range of 0~4.2 V, which is three times that of a single supercapacitor. And the inset of Fig. 7a reveals that the voltage output of such a three in-series

supercapacitor group is high enough to light up a green light emitting diode (LED) when fully charged. However, the total current decreases because of the overlying cell resistance from three supercapacitors. In addition, with the parallel connection (Fig. 7b), a large output current can be realised and satisfy the high current requirement of electrical devices.

4. Conclusions

In summary, a high performance supercapacitor is fabricated by exploiting activated carbon as the electrode and toughened redox-active PVA (polyvinyl alcohol)-H_2SO_4-AQQS (1-anthraquinone sulfonic acid sodium) gel polymer as both electrolyte and separator. The obtained gel polymer possesses not only excellent mechanical strength but also high ionic conductivity. Meanwhile, the as-fabricated supercapacitor with a wide voltage range of 0~1.4 V exhibits outstanding electrochemical performance such as a large specific capacitance (448 F g^{-1}), a remarkably high energy density (30.5 Wh kg^{-1}) and good cycling stability. Moreover, the capacitance of the supercapacitor was maintained very well when the gel electrolyte under various strain conditions (stretching, folding and compressing). The results afforded a facile and efficient way to fabricate supercapacitors based on robust redox-active gel polymer electrolyte for the increasing demands on the high-performance flexible energy storage devices.

Acknowledgements

This research was financially supported by the National Science Foundation of China (Nos. 21164009 and 21174114), the program for Changjiang Scholars and Innovative Research Team in University (IRT15R56), the China Postdoctoral Science Foundation (2013M540778), Key Laboratory of Eco-Environment-Related Polymer Materials (Northwest Normal University) of Ministry of Education, and Key Laboratory of Polymer Materials of Gansu Province.

References

[1] Y. Li, J. Chen, L. Huang, C. Li, J.-D. Hong and G. Shi, *Adv. Mater.*, 2014, **26**, 4789-4793.

[2] S. Wagner and S. Bauer, *MRS Bull.*, 2012, **37**, 207-213.

[3] H. Hu, Z. Zhao, W. Wan, Y. Gogotsi and J. Qiu, *Adv. Mater.*, 2013, **25**, 2219-2223.

[4] B. C. K. Tee, C. Wang, R. Allen and Z. N. Bao, *Nat. Nanotechnol.*, 2012, **7**, 825-832.

[5] Y. Zhu and F. Xu, *Adv. Mater.*, 2012, **24**, 1073-1077.

[6] C. Hou, H. Wang, Q. Zhang, Y. Li and M. Zhu, *Adv. Mater.*, 2014, **26**, 5018-5024.

[7] Y. Zhang, Y. Huang, T. Zhang, H. Chang, P. Xiao, H. Chen, Z. Huang and Y. Chen, *Adv. Mater.*, 2015, **27**, 2049-2053.

[8] X. W. Yang, C. Cheng, Y. F. Wang, L. Qiu and D. Li, Science, 2013, **341**, 534-537.

[9] E. Lim, H. Kim, C. Jo, J. Chun, K. Ku, S. Kim, H. I. Lee, I.-S. Nam, S. Yoon, K. Kang and J. Lee, *ACS Nano*, 2014, **8**, 8968-8978.

[10] Z. Weng, F. Li, D.-W. Wang, L. Wen and H.-M. Cheng, *Angew. Chem. Int. Ed.*, 2013, **52**, 3722-3725.

[11] G. Wang, H. Wang, X. Lu, Y. Ling, M. Yu, T. Zhai, Y. Tong and Y. Li, *Adv. Mater.*, 2014, **26**, 2676-2682.

[12] V. L. Pushparaj, M. M. Shaijumon, A. Kumar, S. Murugesan, L. Ci, R. Vajtai, R. J. Linhardt, O. Nalamasu and P. M. Ajayan, *Proc. Natl. Acad. Sci.*, 2007, **104**, 13574-13577.

[13] J. F. Zang, C. Y. Cao, Y. Y. Feng, J. Liu and X. H. Zhao, *Sci. Rep.*, 2014, **4**, 6492.

[14] M.-Q. Zhao, C. E. Ren, Z. Ling, M. R. Lukatskaya, C. Zhang, K. L. Van Aken, M. W. Barsoum, Y. Gogotsi, *Adv. Mater.*, 2015, **27**, 339-345.

[15] C. Z. Meng, C. H. Liu, L. Z. Chen, C. H. Hu and S. S. Fan, *Nano Lett.*, 2010, **10**, 4025-4031.

[16] L. Huang, D. Chen, Y. Ding, S. Feng, Z. L. Wang and M. Liu, *Nano Lett*., 2013, **13**, 3135-3139.

[17] L. B. Hu, J. W. Choi, Y. Yang, S. Jeong, F. La Mantia, L. F. Cui and Y. Cui, *Proc. Natl. Acad. Sci*., 2009, **106**, 21490-21494.

[18] K. Wang, P. Zhao, X. M. Zhou, H. P. Wu and Z. X. Wei, *J. Mater. Chem*., 2011, **21**, 16373-16378.

[19] W. Chen, R. B. Rakhi, L. Hu, X. Xie, Y. Cui and H. N. Alshareef, *Nano Lett*., 2011, **11**, 5165-5172.

[20] H. Gao and K. Lian, *RSC Adv*., 2014, **4**, 33091-33113.

[21] A. Guiseppi-Elie, *Biomaterials*, 2010, **31**, 2701-2716.

[22] N. A. Choudhury, S. Sampath and A. K. Shukla, *Energy Environ. Sci*., 2009, **2**, 55-67.

[23] P. Simon and Y. Gogotsi, *Nat. Mater*., 2008, **7**, 845-854.

[24] S. T. Senthilkumar, R. K. Selvan, J. S. Melo and C. Sanjeeviraja, *ACS Appl. Mater. Interfaces*, 2013, **5**, 10541-10550.

[25] H. Yu, J. Wu, L. Fan, K. Xu, X. Zhong, Y. Lin and J. Lin, *Electrochim. Acta*, 2011, **56**, 6881-6886.

[26] H. Yu, J. Wu, L. Fan, Y. Lin, K. Xu, Z. Tang and Z. Lan, *J. Power Sources*, 2012, **198**, 402-407.

[27] X. Yang, F. Zhang, L. Zhang, T. Zhang, Y. Huang and Y. Chen, *Adv. Funct. Mater.*, 2013, **23**, 3353-3360.

[28] J. Y. Sun, X. Zhao, W. R. K. Illeperuma, O. Chaudhuri, K. H. Oh, D. J. Mooney, J. J. Vlassak and Z. Suo, *Nature*, 2012, **489**, 133-136.

[29] P. Calvert, *Adv. Mater.*, 2009, **21**, 743-756.

[30] S. Roldan, C. Blanco, M. Granda, R. Menendez and R. Santamarıa, *Angew. Chem. Int. Ed.*, 2011, **50**, 1699-1701.

[31] L. Q. Fan, J. Zhong, J. H. Wu, J. M. Lin and Y. F. Huang, *J. Mater. Chem. A*, 2014, **2**, 9011-9014.

[32] S. T. Senthilkumar, R. K. Selvan, Y. S. Lee and J. S. Melo, *J. Mater. Chem. A*, 2013, **1**, 1086-1095.

[33] S. T. Senthilkumar, R. K. Selvan, N. Ponpandian, J. S. Melo and Y. S. Lee, *J. Mater. Chem. A*, 2013, **1**, 7913-7919.

[34] J. Wu, H. Yu, L. Fan, G. Luo, J. Lin and M. Huang, *J. Mater. Chem*, 2012, **22**, 19025-19030.

[35] Y. Tian, R. Xue, X. Zhou, Z. Liu and L. Huang, *Electrochim. Acta*, 2015, **152**, 135-139.

[36] F. Yu, M. Huang, J. Wu, Z. Qiu, L. Fan, J. Lin and Y. Lin, *J. Appl. Polym. Sci.* 2014, **131**.

[37] J. Zhong, L. Q. Fan, X. Wu, J. H. Wu, G. J. Liu, J. M. Lin and Y. L. Wei, *Electrochim. Acta*, **2015**, 166, 150-156.

[38] J. Zhang, J. Jiang, H. Li and X. S. Zhao, *Energy Environ. Sci.*, 2011, **4**, 4009-4015.

[39] P. C. Chen, G. Shen, Y. Shi, H. Chen and C. Zhou, *ACS nano*, 2010, **4**, 4403-4411.

[40] S. J. Zhu, J. Zhang, J. J. Ma, Y. X. Zhang and K. X. Yao, *J. Power Sources*, 2015, **278**, 555-561.

[41] Y. Li, N. Yu, P. Yan, Y. Li, X. Zhou, S. Chen and Z. Fan, *J. Power Sources*, 2015, **300**, 309-317.

[42] J. Liu, Zhang, L.; Wu, H. B.; Lin, J.; Shen, Z.; Lou, X. W. D. Energy Environ. Sci. 2014, **7**, 3709-3719.

Figure caption

Fig. 1. FE-SEM images of activated carbon under different magnifications.

Fig. 2. (a) Tensile property of PHA gel polymer before and after electrochemical tests. (b) Twist demo of PHA gel polymer. (c) Compression property of PHA gel polymer. (e-f) The schematic diagram of fabricated supercapacitor with PHA gel film and its flexible behavior.

Fig. 3. (a) CV curves of supercapacitors in 1 M H_2SO_4, PH and PHA electrolyte at scan rate of 10 mV s^{-1}. (b) CV curves of the supercapacitor with PHA gel film at different scan rates. (c) The C_s of supercapacitors with PVA-H_2SO_4-AQSS gel films contained different AQQS contents at a current density of 0.5 A g^{-1}. (d) Nyquist impedance plots of supercapacitors based on PVA-H_2SO_4-AQSS gel films with various AQQS contents.

Fig. 4. (a) GCD curves of supercapacitors with PH and PHA gel films at a current density of 0.5 A g^{-1}. (b) GCD curves of the supercapacitor with PHA gel film at various current densities. (c) The C_s of supercapacitors with PH and PHA gel films at various current densities. (d) Ragone plots related to energy and power density of supercapacitors with PH and PHA gel films.

Fig. 5. (a) Nyquist impedance plots of supercapacitors with PH and PHA gel films, the inset showed an equivalent circuit used to fit the Nyquist spectra. (b) Cycle life performance of the supercapacitor with PHA gel film tested at a constant current density of 1 A g^{-1} as a function of cycle number, and the inset is CV curves of the supercapacitor with PHA gel film at the 1^{st} and 1000^{th} cycles.

Fig. 6. (a) The C_s of the supercapacitor applying PHA gel film with various stretching state at the current density of 1 A g^{-1}, and the inset is GCD curves of the supercapacitor when the gel film under 0% and 100% stretching strains. (b) CV curves of the supercapacitor with PHA gel film under flat and fold conditions at the scan rate of 25 mV s^{-1}. (c) The C_s of supercapacitor with PHA gel film under fold states at various current densities. (d) The C_s of the supercapacitor with PHA gel film under various compressive stresses at the current density of 0.5 A g^{-1}.

Fig. 7. (a) The CV curves of a three in-series supercapacitor group and a single supercapacitor at the scan rate of 25 mV s^{-1}, and the inset shows a green LED was powered by three charged serial supercapacitors. (b) CV curves collected at the scan rate of 25 mV s^{-1} of a three in-parallel supercapacitor group and a single supercapacitor, the insert is the circuit diagram of the parallel connection of three supercapacitors.

Table 1 Fitted impedance parameters based on the proposed equivalent circuit and some of the other characteristic parameters of supercapacitors with PH and PHA gel films.

Table 2 Comparison of energy density with different reported values.

Fig. 1

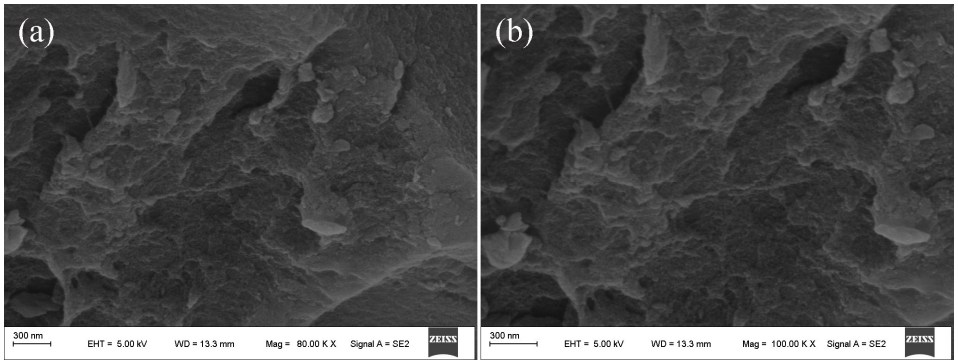

Fig. 2

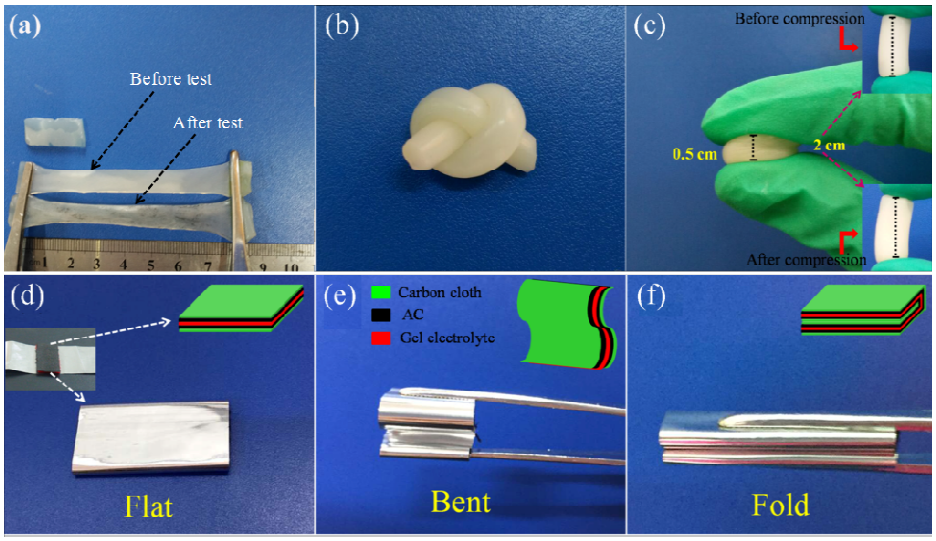

Fig. 3

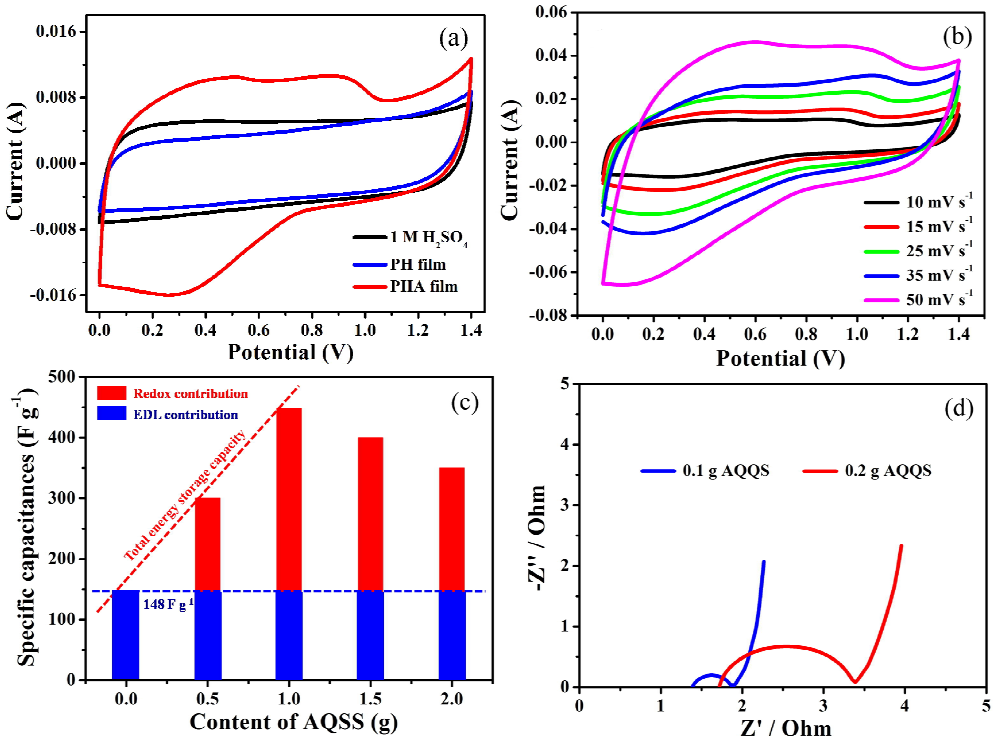

Fig. 4

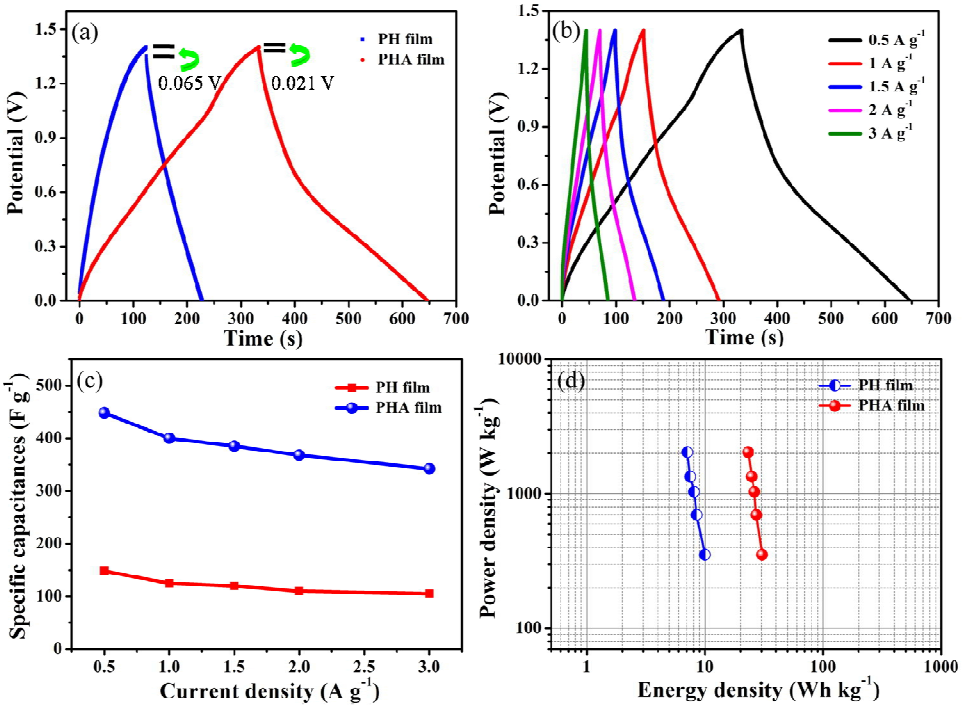

Fig. 5

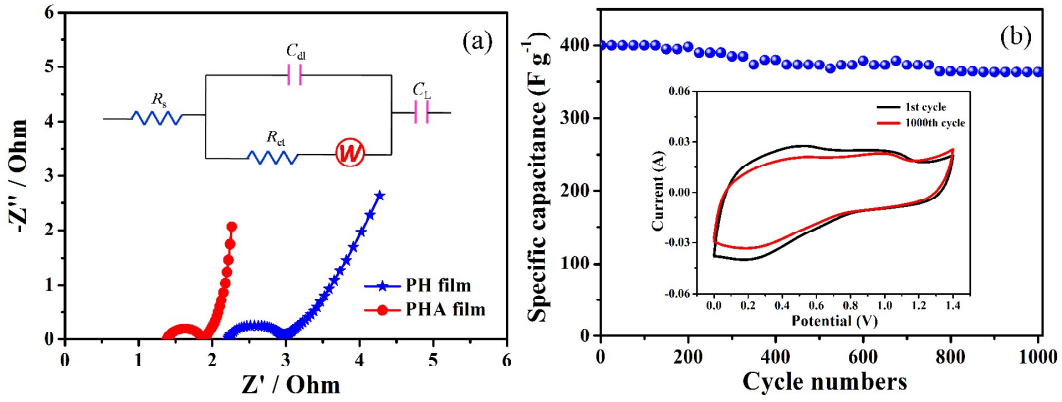

Fig. 6

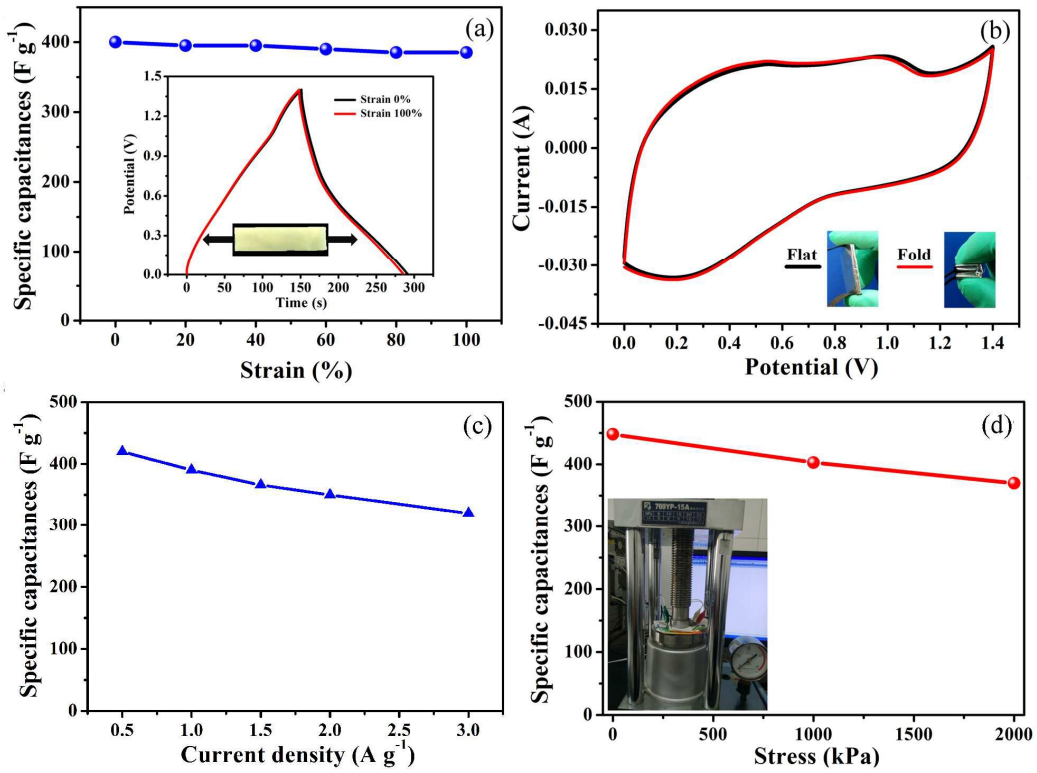

Fig. 7

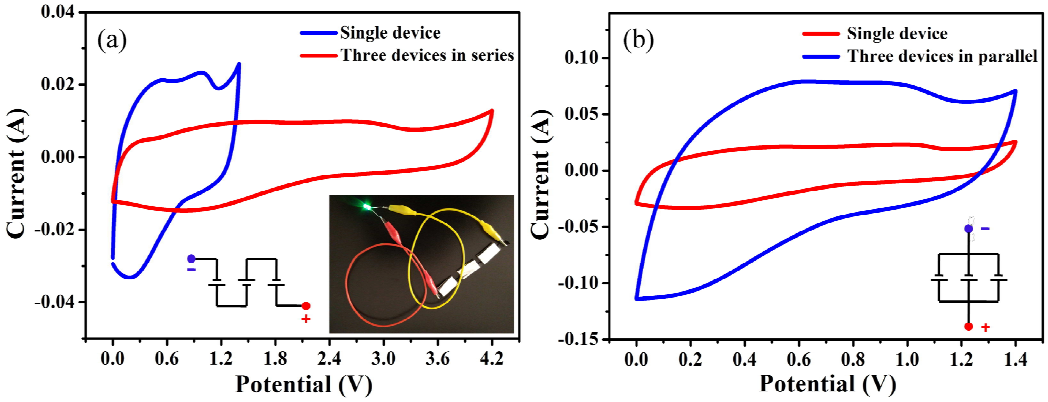

Table 1

Electrolyte	R_s/Ω cm^2	R_{ct}/Ω cm^2	C_{dl}/mF cm^{-2}	A_w/Ω $s^{-1/2}$ cm^2	C_L/F cm^{-2}	ESR/Ω cm^2	σ/mS cm^{-1}
PH	2.24	0.73	0.28	0.72	0.18	9.02	15.7
PHA	1.42	0.36	0.22	0.31	0.54	2.90	28.5

Table 2

Electrode material	Electrolyte	Conditions	Energy density/Wh kg^{-1}	Ref.
Activated carbon	H_2SO_4 + KI	2 mA cm^{-2}	19.04	32
Activated carbon	H_2SO_4 + $VOSO_4$	1 mA cm^{-2}	13.7	33
Activated carbon	KOH + p-phenylenediamine	1 A g^{-1}	19.86	34
Activated carbon	KNO_3 + anthraquinone-2,7-disulphonate	1 A g^{-1}	21.2	35
Activated carbon	PVA-KOH + KI	0.8 A g^{-1}	15.34	25
Activated carbon	PVA-PVP-H_2SO_4 + methylene blue	1 A g^{-1}	10.3	36
Activated carbon	PVA-H_2SO_4 + Na_2MoO_4	1.56 A g^{-1}	14.4	24
Activated carbon	PVA-H_2SO_4 + KI + $VOSO_4$	0.5 A g^{-1}	25.4	31
Activated carbon	PVA-H_2SO_4 + methylene blue‖ PVA-H_2SO_4 + hydroquinone	0.5 A g^{-1}	18.7	37
Activated carbon	PVA-H_2SO_4 + 1-anthraquinone sulfonic acid sodium	0.5 A g^{-1}	30.5	This work

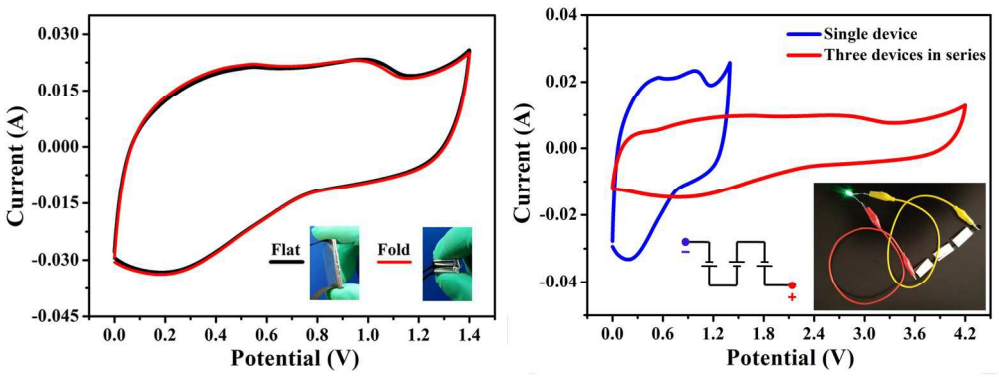

361x134mm (150 x 150 DPI)